AD-A188 988 DYNAMICS OF PRODUCTION AND OXIDATION OF ORANES(U) 1/1
CORNELL UNIV ITHACA NY DEPT OF CHEMISTRY S H BAUER
01 DEC 87 ARO-21968 3-CH DAAG29-84-K-0195

UNCLASSIFIED F/G 7/4 NL

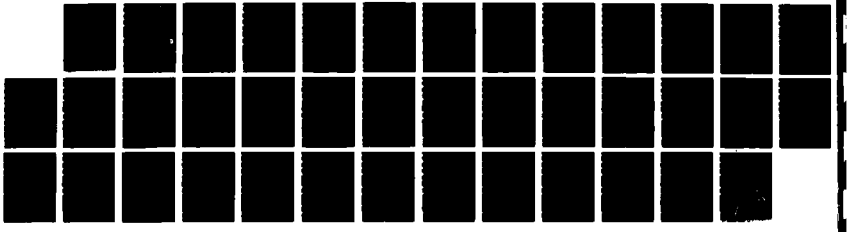

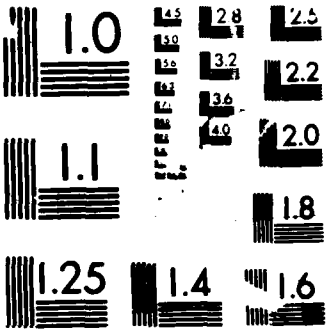

MICROCOPY RESOLUTION TEST CHART
OS-1963-A

REPORT DOCUMENTATION PAGE

READ INSTRUCTIONS BEFORE COMPLETING FORM

1. REPORT NUMBER: ARO 21968.3-CH
2. GOVT ACCESSION NO.:
3. RECIPIENT'S CATALOG NUMBER:

4. TITLE (and Subtitle): Dynamics of Production and Oxidation of Boranes
5. TYPE OF REPORT & PERIOD COVERED: FINAL 12/04/84 - 10/01/87
6. PERFORMING ORG. REPORT NUMBER:

7. AUTHOR(s): Simon H. Bauer
8. CONTRACT OR GRANT NUMBER(s): DAAG29-84-K-0195

9. PERFORMING ORGANIZATION NAME AND ADDRESS:
Department of Chemistry
Cornell University
Ithaca, New York 14853-1301
10. PROGRAM ELEMENT, PROJECT, TASK AREA & WORK UNIT NUMBERS:

11. CONTROLLING OFFICE NAME AND ADDRESS:
U. S. Army Research Office
Post Office Box 12211
Research Triangle Park, NC 27709
12. REPORT DATE: 12/01/87
13. NUMBER OF PAGES: 35

14. MONITORING AGENCY NAME & ADDRESS (if different from Controlling Office):
15. SECURITY CLASS. (of this report): Unclassified
15a. DECLASSIFICATION/DOWNGRADING SCHEDULE:

16. DISTRIBUTION STATEMENT (of this Report)

Approved for public release; distribution unlimited.

17. DISTRIBUTION STATEMENT (of the abstract entered in Block 20, if different from Report)

NA

18. SUPPLEMENTARY NOTES

The view, opinions, and/or findings contained in this report are those of the author(s) and should not be construed as an official Department of the Army position, policy, or decision, unless so designated by other documentation

19. KEY WORDS (Continue on reverse side if necessary and identify by block number)

Boranes
Combustion
Laser Induced Fluorescence
Oxygen atoms
Flow tube reactor
Kinetic mechanism

20. ABSTRACT (Continue on reverse side if necessary and identify by block number)

We measured, via LIF, time-dependent concentrations of OH resulting from the reaction of $O(^3P)$ with B_2H_6 and C_2H_6. The oxygen atoms were generated by titrating microwave discharged N_2/He with NO to the chemiluminescent end-point. The operating pressures in the flow reactor ranged from 5 to 15 torr; the mixtures consisted of He/$O(^3P)$/fuel in the approximate ratios 100/1/0.1 to 100/1/1. Flow conditions were such that in the low pressure experiments the controlled residence time prior to detection were 0.8-17 ms; under the higher pressure conditions, the time interval covered was 2-37 ms. We estimated that the temperature of the

reaction region was ≈350K, based on rotational emission temperatures measured for BO*, generated under closely similar conditions. First a complete mechanism was derived for ethane for a specified set of experimental parameters. For ethane, a single set of experimental conditions was selected for ratioing the recorded intensity to the computed OH density; this was cross-checked with other runs for ethane. Finally, a mechanism was developed for B_2H_6, which quantitatively checked our experimentally determined profiles both in shape and magnitude, for three sets of conditions, and within a factor of two for the high concentration runs (100% B_2H_6 feeding into the reactor at 14 Torr).

TABLE OF CONTENTS

OBJECTIVES:

a) To develop general mechanisms for the reactions of low molecular weight boranes with atomic oxygen [O(^{3}P)] at ambient temperatures.

b) To utilize, as the principal diagnostic, laser induced fluorescence of the dominant product species [OH], rather than measure overall rates of disappearance of the reactants.

c) To estimate rate constants for the dominant reactions in the multi-step mechanism, comparable to those available for the combustion of low molecular weight hydrocarbons.

SUMMARY OF RESULTS:

a) A low pressure flow-tube reactor was set up; this provided controlled flow rates of measured levels of oxygen atoms and of fuels.

b) A Nd/YAG/Dye laser system was set up for generating pulses of 307.93 nm radiation, to excite the ground state OH to its A state, from which it fluoresces.

c) A fluorescence radiation detection, recording and data processing system was assembled. Initially we use a boxcar integrator. Subsequently, we switched to a Biomation digitizer, reading into a dual channel Tracor-Northern, and into a computer.

d) Appropriate thermochemical and kinetics codes were assembled and made compatible with our computers. The available codes were extended and tested.

e) Numerous preliminary experiments were run with various hydrocarbons. Ultimately C_2H_6 + O(^{3}P) was selected for calibrating the output signal, so that fluorescence intensities measured for B/H compounds could be converted quantitatively to [OH] levels, in (moles/liter) at the intersection point of the sampling jet with the laser beam.

f) A self-consistent, quantitatively scalable mechanism was developed for the reaction of ethane with oxygen atoms.

g) An adequate mechanism was developed for the reaction of diborane with oxygen atoms.

h) Preliminary relative rates of OH production from several interesting hydrocarbons were obtained.

i) Preliminary rates of OH production from the reaction of O(^{3}P) with H_3BCO and B_4H_9 were recorded.

PERSONNEL: Post Doctoral Associates

Jong-Gill Choi: Ph.D., Brown University [12/04/84 - 02/14/87]

Dan B. Borchardt: Ph.D., Washington State [02/15/87 - 10/01/87]

PUBLISHED:

The Gas Phase Kinetics of Boron and Borane - A Review, Chapter 19, in Molecular Structure and Energetics, Vol. 5 (1987), Ed. J. F. Liebman and R. Williams.

HYDROGEN ATOM ABSTRACTION BY O(³P) FROM DIBORANE AND ETHANE

D. B. Borchardt, J-G. Choi*, K. Suzuki† and S. H. Bauer

Department of Chemistry, Baker Laboratory

Cornell University, Ithaca, New York 14853

ABSTRACT

We measured, via LIF, time-dependent concentrations of OH resulting from the reaction of O(³P) with B_2H_6 and C_2H_6. The oxygen atoms were generated by titrating microwave discharged N_2/He with NO to the chemiluminescent end-point. The operating pressures in the flow reactor ranged from 5 to 15 torr; the mixtures consisted of He/O(³P)/fuel in the approximate ratios 100/1/0.1 to 100/1/1. Flow conditions were such that in the low pressure experiments the controlled residence time prior to detection were 0.8-17 ms; under the higher pressure conditions, the time interval covered was 2-35 ms. We estimated that the temperature of the reaction region was ≈350K, based on rotational emission temperatures measured for BO, generated under closely similar conditions. First a complete mechanism was derived for ethane for a specified set of experimental parameters. For ethane, a single set of experimental conditions was selected for ratioing the recorded intensity to the computed OH density; this was cross-checked with other runs for ethane. Finally, a mechanism was developed for B_2H_6, which quantitatively checked our experimentally determined profiles both in shape and magnitude, for three sets of conditions, and within a factor of two for the high concentration runs (100% B_2H_6 feeding into the reactor at 14 Torr).

†Permanent address: Department of Chemistry, Faculty of Science, University of Tokyo, Hongo, Bunkyo-ku Tokyo 113 Japan

*Permanent address: Korean Research Institute of Chemical Technology, P. O. Box 9, Daedeog-Danji, Chungnam, Korea 300-31

INTRODUCTION

The common charcteristics of oxidations of boron hydrides and related compounds are rapid rates, large exothermicities, and strong visible and ultraviolet chemiluminescence. These features lead to the expectation that the reaction may generate products in nonthermal distributions, and possibly could be used to construct chemical lasers at visible wavelengths. General reviews of reactions between molecular oxygen and diborane date back to reports by Berl[1] and by Bauer and Wiberley[2]. The reaction between diborane and atomic oxygen was initially studied by Hand and Derr[3] in a flow-tube reactor. More recently, Anderson and Bauer[4] measured the rates of attack of B_2H_6 and H_3BCO by O and N atoms under rapid-mixing fast-flow conditions, using direct sampling by a TOF mass spectrometer. The dynamics of reaction between oxygen atoms and borane trimethylamine, based on spectral analysis of the chemiluminescence were described by Jeffers and Bauer.[5,6] Although considerable information is available on the chemistry of boranes[7], the complex mechanism operating during O atom attack, other than the total rate of destruction of the borane, has not been formulated except in a theoretical paper by Shaub and Lin.[8]

The importance of fully characterizing the reactions of fuels with $O(^3P)$ and with $OH(^2\Pi_i)$ can be judged from the vast literature on these reactions which has accumulated during the past fifteen years. For oxygen-atom attack on alkanes a current summary has been prepared by Cohen.[9] Earlier reviews were assembled by Herron and Huie.[10] There is total agreement that the primary products are alkyl radicals and OH. The vibrational state distribution of the hydroxyl radicals increases in the sequence: primary → secondary → tertiary (as do the corresponding exothermicities), whereas the rotational

state distribution appears to be independent of the type of hydrogen which has been abstracted[11], with relatively little energy deposited in rotation. These observations are consistent with a co-linear "three atom" model [R--H--O] for the transition structure.[12] The energies of activation range from 7.3 kcal/mol for straight chain primary H's to 2.5 kcal/mol for tertiary H's; the entropies of activation (298K) span the interval -19.2 to -22.7 e.u., depending on the number and types of hydrogens present. Typically $k(298) \approx 10^{11}$ $mol^{-1}cm^3s^{-1}$.

The abstraction of H atoms from alkanes by OH radicals follows a similar pattern. An extended review was prepared by Atkinson, et al.[13] about seven years ago. Cohen's significant procedure for extrapolating the available experimental data to higher temperatures[14] (as required for combustion applications) was recently implemented by Walker[15] for the range 300-1000K. The entropies of activation are generally higher than for oxygen atom attack (-23 to -27 e.u.), but the rate constants are larger, typically $k(298) \approx 10^{12.5}$ mol^{-1} cm^3 s^{-1}. These are comparable to rate constants for the gas phase abstraction of hydrogens by chlorine atoms.[16]

A general feature of the kinetic measurements is that they were made under conditions in which one species was present in large excess over the other, so as to minimize complications due to secondary reactions. Recently, however, it has been pointed out by Cohen[17] that in alkane + $O(^3P)$ reactions, the measured values are particularly sensitive to errors introduced by uncounted secondary reactions and by low levels of impurities. Detailed discussions of chemical kinetic modeling of hydrocarbon oxidation under combustion conditions was reviewed by Westbrook and Dryer.[18]

It is evident that until rates of <u>production</u> of specific species are determined, overall mechanisms cannot be established. In this report we pre-

sent time-dependent OH concentrations generated under a variety of initial conditions, upon mixing excess $O(^3P)$ with diborane, based on the reaction $[C_2H_6 + O(^3P)]$ for calibration of our experimental protocol. The products of a fast-flow reactor were sampled via LIF by OH. Dutton, et al.[19] adopted the LIF technique for determining dynamics of the OH produced in molecular beams, for the abstraction from hydrocarbons, cyclic hydrocarbons, and ethanol. Their observations indicated that the abstraction is a direct step and takes place only when the oxygen atom is collinear with the C-H bond under attack. In our experiments $OH(A^2\Sigma^+ - X^2\Pi_i)$ fluorescence intensities for all runs were measured under strictly comparable conditions and reduced to absolute OH concentrations by ratioing the computed value to the measured fluorescence intensity at a single experimental point from an extended run for C_2H_6, assuming that the proposed mechanism for ethane is quantitatively correct. The internal consistency of this assumption is demonstrated below. Computational simulations were developed, and the time dependent concentrations were compared with the experimental values. Thus, we derived the "best" estimates for the rate coefficients at the temperature of the flow medium, which is in the vicinity of 350K, based on the rotational temperature determined in a similar flow system.[6]

EXPERIMENTAL

Figure 1 is a schematic of the apparatus. It consists of a microwave discharge arm, a flow reactor, and a detection chamber. The reactor is a pyrex tube 2.5 cm in diameter (upper part) and 1.25 cm (lower part), with a 30 cm long reaction zone. Atomic species are generated in a microwave discharge and injected into the reaction zone through the side arm, as indicated.

Samples of fuel are introduced through a 0.63 cm I.D. pyrex tube, which can be slid along the axis of the reactor to change the mixing region relative to the sampling pin-hole. The reactor is evacuated by a fast mechanical pump; the pressure in the reactor can be controlled and maintained at 1-15 torr, depending on the opening of the valve. The sampling pin-hole is 0.50 mm. That section of the apparatus was constructed following the design developed by Anderson and Bauer[4]. The reactions products expand under near-continuum flow through the skimmer into the detection region. With this configuration the molecular densities measured are the concentrations developed along the central streamline. The stainless steel detection chamber is evacuated by a 10 cm oil diffusion pump; the background pressure in the detection area is maintained at $<10^{-3}$ torr.

The hydroxyl radicals are detected by laser induced fluorescence of OH [$A^2\Sigma \leftarrow X^2\Pi$] at the (0,0) band, for the $Q_1(1)$ transition (307.9 nm). A Nd:YAG laser (Quanta-Ray DCR), operating at a repetition rate of 10 Hz, pumps a Quanta-Ray PDL-1 pulsed dye laser, (sulforhodamin 101). Its output is frequency-doubled with a KDP crystal (Quanta-Ray crystal module-1) to produce a maximum pulse energy of about 1 mJ at 308 nm and a bandwidth of ≈0.1 nm FWHM. The laser beam passes through a visible light rejection filter, an iris and through a lens which focuses it onto the well-defined jet that emerges from the skimmer. The entrance and exit quartz windows are set at the Brewster angle. To minimize scattered laser light a series of baffles were inserted in long arms, and the walls of the vacuum chamber were painted black. On exit a portion of the direct beam is monitored with a photomultiplier. The fluorescence signal is detected by a EMI 6256B photomultiplier set at right angles with respect to both the directions of the laser beam and the jet. A filter (Hoya 4340) was mounted in front of the photomultiplier to

reject wavelengths outside the region 275-375 nm. Initially the output of a box-car integrator, operating with a gate width of 5 μs, was recorded and averaged graphically. However, the incorporated background levels comprised the major part of the signal. More reliable data are obtained (as indicated in Fig. 1) with a Biomation digitizer (10 ns/pt) reading into a dual channel Tracor-Northern, which is set to subtract the background profile (recorded immediately prior to each run) from the fluorescence profile. The first ≈100 ns of the scattered light signal are not recorded. The exponential decay curve from $OH(A^2\Sigma^+)$ is plotted and digitally integrated to generate a single point for each combination of experimental parameters.

Ground state oxygen atoms are produced by visual titration with NO of discharged (N_2+He), which passes through the microwave cavity; this yields a stream of O atoms free of O_2. The rates of the gas flow are monitored by a series of metering valves and flow meters, which were calibrated by measuring the rates of pressure decrease in known volumes. Under typical experimental condition, the flow rates of the gases are: 1.43 μmol/s (for C_2H_6), 3.62 μmol/s (for NO), 196 μmol/s (for N_2), and 336 μmol/s (for He), at a flow reactor pressure (total) of 7 torr. The linear flow speed of the sample was calculated to be 2.1×10^3 cm/s, so that the shortest dwell time in the reactor is about 0.8 ms; the longest time can be extended to ≈17 ms for reactor pressure at 7 torr, and to 35 ms at 14 torr.

The stock gases used in these studies were obtained from AIRCO for N_2 (99.995%), He (99.995%), and Ar (99.998%), and from Matheson for NO (cp, 99.0% min). This gas was purified by trap-to-trap distillation prior to use. To check for impurities in C_2H_6, the gas was injected onto an FID gas chromatograph (F&M Scientific Co., Model 810) with a GC column consisting of 20% carbowax 20M on 100/120 supelcoport. The total impurity level was found to be

less than one part per thousand (<0.1%). Diborane was prepared by the action of 85% phosphoric acid on $NaBH_4$. It was separated from other products (mostly H_2 and Na_3PO_4) by successive distillation, and collected in a LN_2 trap. The FTIR spectrum of diborane purified by this procedure showed no impurities. The B_2H_6 was stored at -196°C and redistilled immediately before use. Vapors of the fuels were mixed with He (baromatic mixing) to obtain the desired concentrations. In contrast to data sets recorded with ethane, which were highly reproducible, runs with diborane showed irreproducibilities (±20%). These fluctuations were minimized by careful cleaning and drying of the flow-reactor tube every 3-5 runs.

An intense blue chemiluminescence was observed with diborane, due to the formation of BO*.[4,5] Its intensity increased with the concentration of the hydride. This cool blue emission consists of BO-$^{\alpha}$ bands ($A^2\Pi \rightarrow X^2\Sigma^+$), and is generated by the reaction of oxygen atoms with BH, and possibly with BH_2.[5,6]

EXPERIMENTAL PROCEDURES; INTENSITY CALIBRATION

When the dye laser output was scanned over a 0.3 nm on either side of 307.9 nm, fluorescence from OH, generated by reaction between the fuel and $O(^3P)$, appears as sharp line features, assigned to $Q_1(1)$ at 307.93; $Q_1(2)$ at 308.09 nm. The recorded intensity developed at a selected transition can be changed by rotating the doubling KDP crystal to maximize the laser power at the desired resonance frequency. In view of the constant low levels of exciting radiation quenching effects are negligible. Intensities were recorded for different positions of the injecting tube to develop temporal profiles of OH concentrations. For each fuel several sets of experiments were

performed at two total pressures, set at 7 or 14 torr. The pressure in the reactor was varied by changing the aperture of the valve which connects the reactor tube to the mechanical pump, so that concentrations of the sample and of the oxygen atoms were changed by the same amount. C_2H_6 shows a linear increase with pressure, as expected for a bimolecular reaction with a modest rate constant; also B_2H_6 was demonstrated to show a linear response to flow rate.

The following strategy was developed to obtain a quantitative relation between the magnitudes of integrated fluorescence signals and the corresponding concentrations of OH (mol ℓ^{-1}) at the intersection of the laser beam with the jet, which samples the central stream within the flow reactor.

(a) A set of reactions and rate constants (at 300 K) for [C_2H_6 + $O(^3P)$] were assumed, based on numerous literature reports. These were slightly adjusted (see below) until the computed $[OH]_t$ coincided with the observed profiles, and precisely scaled with operating pressure and reactant concentrations (Fig. 2).

(b) For a selected set of experimental conditions three computed points were identified with corresponding signal levels, and their ratio averaged, thus providing a factor that relates [OH] to the recorded signal.

(c) Immediately before and directly after a run with another fuel, reference runs with ethane were recorded, with all experimental parameters such as laser intensity, flow rates and operating pressures kept constant.

(d) In view of the comparable levels of incident laser intensity and recorded fluorescence for C_2H_6 and B_2H_6, small saturation effects, if present, cancel.

DETAILS OF MECHANISM

A general kinetics code developed at NBS[20] was expanded by Dr. N-S. Chiu in several respects. The program requires only that the reacting species be specified, their reactions listed, and for each a rate constant inserted (for a fixed temperature run). One then obtains a print-out of: (a) the concentration of each of the species as a function of time; (b) the rates of each reaction as a function of time; (c) the Jacobian for any selected species relative to all the other at selected (prespecified) times; in our case, $d\{\partial[OH]/\partial t\}/d[X]$. These provide direct measures of the sensitivity of the species of interest to inclusions of other species and of plausible reactions. 50 species and 200 reaction rates can be integrated.

The calculations were carried out to simulate our experimental parameters. A set of 67 of the most plausible reactions needed to describe the evolution of the systems $O(^3P)$ with C_2H_6 were used. The initial concentrations of the reactants were calculated from measured flow rates. These ranged from 8.3×10^{-7} to 3.2×10^{-6} mol/ℓ for ethane and 1.4×10^{-6} to 1.7×10^{-6} mol/ℓ for oxygen atoms, with total pressures 7 to 14 Torr. Note that in the reactor the major constituent was helium (at about 3×10^{-4} mol/ℓ) so that the reactants were present at roughly 1/100 of that level.

Under our experimental conditions, the initial abstraction step

$$O + C_2H_6 \longrightarrow C_2H_5 + OH$$

is rapidly followed by many secondary and tertiary processes. A model consisting of 30 species, participating in 67 reactions, was assembled and integrated to generate the OH concentration profiles. It soon became evident that only 16 species were essential and the number of reactions was reduced to 29, presented in Table I. Winnowing was achieved by carefully examining the com-

puter outputs. We found that the concentration of each species at corresponding time scales were within 10% of those calculated with the larger set (67 reactions). It is significant to note that at low temperatures 13 reactions (#3 to #15) appear in all H/O systems. The time dependent concentrations of OH are very sensitive to these rate constants. Since they are present in all low pressure and low temperature flames for hydrogenic fuels these thirteen reactions were incorporated (unaltered) in every mechanism, as listed in Table I.

The rate constants used in the simulations were selected primarily from Refs. 21 and 22. A few of the rate constants were estimated from analogous reactions. Several were subjected to reasonable revisions, required to obtain fits between the computed and absolute magnitudes, as well as the time dependent OH concentrations, with those observed. For three-body reactions [#3, 5, 6, 7, 9, 10, and 11] *corresponding* 2-body rate constants were obtained by multiplying the 3-body values by the concentration of M at the corresponding a reactor pressure. Also, since there are no ambient temperature values available for reactions #5, 6, and 9, we inserted somewhat larger values than those reported for high temperatures. This is justified in view of the demonstrated negative temperature dependence (T^{-1} to $T^{-1.5}$) for termolecular associations with small or zero activation energies.[23] Many small variations in the magnitudes of several rate constants were tested until the best fits between the experiments and the calculations were obtained. Figure 2 shows that by normalizing the observed intensities to 100% C_2H_6 (14 Torr reactor pressure) both it and 100% C_2H_6 (7 Torr reactor pressure) runs are well reproduced over the entire reaction period.

In Table I, OH is generated in reactions #1, 6, 8, 12, 15, 20, 24, and 27, and destroyed in reactions #2, 4, 5, 9, 21, and 25. However, in the early

stages the major production source of OH is #1, and the major consumption step is #4; H atoms and HO_2 radicals play an important controlling role at later times. During the time interval covered by our measurements, the 29 step model shows that the steady state concentration of OH is controlled by several rate processes;

$$[OH]_{ss} = \frac{\sum_i k_i[R_i][O] + \sum_j k_j[R_j][H]}{(k_4 + k_5)[O] + \sum_r k_r[R_r]} \qquad [1]$$

$$= (k_4 + k_5)^{-1} \frac{\sum_i k_i[R_i] + \sum_j k_j[R_j]\{[H]/[O]\}}{1 + \sum_r \{k_r/(k_4+k_5)\}\{[R_r]/[O]\}} \qquad [2]$$

$$\equiv (k_4 + k_5)^{-1} \frac{\alpha + \beta}{1 + \gamma} \qquad [3]$$

where R_i = C_2H_6, H, HO_2, CH_3CHO, HCHO, HCO,

R_j = HO_2, O_3, and

R_r = C_2H_6, H, CH_3CHO and HCHO.

Inspection of the computer print-outs shows that at 7 torr operating pressure, 10 ms residence time, 100% C_2H_6 in He:

$\alpha = 5.57\ s^{-1}$; $\beta = 1.02 \times 10^{-2}\ s^{-1}$; $\gamma = 8.7 \times 10^{-3}$

At 14 torr operating pressure, 10 ms residence time, 100% C_2H_6:

$\alpha = 26.6\ s^{-1}$; $\beta = 0.78\ s^{-1}$; $\gamma = 3.5 \times 10^{-2}$

While these are tightly coupled reactions nonetheless a good estimate of the sensitivity for [OH] production to the various rate constants is obtained from:

$$\frac{\partial[OH]_{SS}}{\partial k_i} = \frac{[R_i]_t}{k_4 + k_5} \qquad [4]$$

These values are listed in Table II at four selected times. The most sensi-

tive rate constant is k_1, but at later times (≈ 15 ms), the [OH] is also significantly controlled by k_6. The destruction of [OH] is primarily controlled by k_4.

$$\frac{\partial[OH]_{SS}}{\partial k_4} = \frac{-a}{[k_4 + k_6]^2} \qquad [5]$$

Besides major consumption of [OH] by reactions (4) and (5), at later times, reactions (9) and (12) assume significant roles.

THE BORANE OXIDATION

A data set essential for providing the rationalé for selecting pertinent reactions to be included in kinetic mechanisms for $B_2H_6 + O(^3P)$ is a table of heats of formation and estimated entropies, of all plausible molecular fragments involving B/O/H. The "best" set, we believe, has been generated by C. F. Melius which we adopted (Appendix). Then, for a list of 15 B/O/H containing species and 9 O/H species we generated a computer printout of all possible unimolecular and bimolecular reactions (allowing for three molecular products as well) in which these 24 species could participate, subject to the mass conservation constraint. Corresponding ΔH^0_{300}, ΔS^0_{300} and ΔG^0_{300} values were calculated for each reaction. The resulting table had over 1000 lines (forward and reverse steps were listed individually). When all reactions with

$\Delta G^0 > -4.0$ kcal/mole were eliminated, the list shrank to 670; further reductions were achieved by eliminating implausible reactions. A final set of 40 pertinent reactions was identified on the basis of numerous trial kinetic runs.

Anderson and Bauer[4] proposed that the magnitudes of the rate constants for attack on borane adducts by oxygen atoms provide a clue for the initial

steps of the oxidation reaction. They also indicated that the mechanism requires the assumption of <u>two</u> initiation routes; one in which the O atom abstracts hydrogen(s) from one BH_3 group while ejecting the opposite BH_3, and the other in which the $O(^3P)$ directly attacks the boron atom. Fehlner and Strong[28] proposed the initiation step is: $B_2H_6 + O(^3P) \rightarrow H_3B + H_3BO$. However, abstraction that leads to BH and BH_2 (followed by the formation of OH radicals) is essential for the subsequent production of $BO(A^2\Pi)$, which is the source of intense chemiluminescence.

The mechanism that best describes the oxidation of B_2H_6 by reproducing our [OH] profiles for several concentrations and flow rates is listed in Table III. In the flow tube reactor with $[B_2H_6]_i = 2.07 \times 10^{-6}$, $[O]_i = 1.11 \times 10^{-6}$ and $[N_2; He]_i = 3.74 \times 10^{-4}$ mol/ℓ, at <u>5 ms</u> after mixing, $[BH_3]_{calc} = 5.71 \times 10^{-10}$; $[OH]_{calc} = 3.30 \times 10^{-10}$; agreement with the observed value is illustrated in Fig. 3B. In the lower graph (3C) note the longer time scale ; here $[B_2H_6]_i = 2.06 \times 10^{-7}$ injected at 14 Torr, 25% diluted in He; $[O]_i = 1.78 \times 10^{-6}$ with $[He,N_2]_i = 7.48 \times 10^{-4}$ mole/ℓ. At 6.94 ms, $[BH_3]_{calc} = 4.84 \times 10^{-10}$, $[OH]_{calc} = 3.28 \times 10^{-10}$, which checks well with the observed profile. We applied two criteria for an acceptable mechanism: a good match between calculated and recorded <u>shapes</u> of the concentration/time profiles, covering the time range 0.8-35 ms, <u>and</u> quantitative checks of the absolute magnitudes of [OH] over a 4-fold concentration range of initial B/H levels. After many, many attempts to select significant reactions and adjust their rate constants, we could not find one set that generates the agreements shown in Fig. 3A,B,C and <u>concurrently</u> accounts for the magnitudes of [OH] recorded when <u>undiluted</u> diborane was injected at 14 Torr {i.e. back pressure corresponds to 7.5×10^{-4} mol/ℓ}. Then, observed levels of OH were about one-half of those calculated. We ascribe this discrepancy in part to

incomplete mixing.

A sensitivity analysis, parallel to that for C_2H_6 shows that the approximate steady state concentration of OH is

$$[OH]_{ss} = (k_{29} + k_{30})^{-1} \frac{\sum_i k_i[R_i] + \sum_j k_j[R_j]\{[H]/[O]\} + \sum_\ell k_\ell[R_\ell][O_2]/[O]}{1 + \sum_r \{k_r/(k_{29}+k_{30})\}\{[R_r]/[O]\}} \quad [6]$$

$$= (k_{29} + k_{30})^{-1} \frac{\alpha + \beta + \theta}{1 + \gamma}$$

where $R_i = B_2H_6$, H, HO_2, BH_3, BH_2, H_2BOH, HBOH, OBOH

$R_j = HO_2$, O_3; and $R_\ell = BH_3$, BH_2, BH.

$R_r = B_2H_6$, H, B_2H_5, BH_3, HBO, BO, BH.

At 7 torr operating pressure, 8.4 ms residence time, for undiluted B_2H_6:

$\alpha = 80.8\ s^{-1}$; $\beta = 1.05\ s^{-1}$; $\theta = 0.023\ s^{-1}$; $\gamma = 0.78\ s^{-1}$.

While one may develop a sensitivity analysis, similar to that for ethane, its significance is of dubious value in view of the many estimated rate constants incorporated in Table III. Inspection of the various magnitudes which contribute to α,β,θ and γ indicates that for [OH] production, reactions (19), (10) and (2) dominate; the destruction of [OH] is controlled primarily by (29), as in the hydrocarbon system.

It is interesting to note that whereas the initiating steps #1 and #2 for $O(^3P)$ with diborane are unique, in general the graphs and the mechanism are analogous to those for C_2H_6 + O. This should not be surprising, since the dissociation energy of a terminal B/H (≈85 kcal/mol) is comparable to that of C/H (≈100, 95, and 92 kcal/mol for primary, secondary, and tertiary bonds, respectively).

CONCLUDING COMMENT

Our experimental OH profiles, along with the model calculations demonstrate that many elementary reactions must be taken into account in order to elucidate the oxidation dynamics of boranes and hydrocarbons. This applies even when the oxidizer/fuel ratio is relatively large. For ethane it is unlikely that small changes in the proposed rate constants will alter the shapes of the OH profiles. We reiterate that in developing the mechanism presented in Table III, about 380 reactions were considered; approximately 100 were tested in various combinations, and more than half were found not to influence the levels of OH, assuming reasonable magnitudes for the corresponding rate constants. We have no basis, at this time, for estimating the relative importance of reactions such as:

$$B_3H_7 + O \rightarrow B_3H_6 + OH$$
$$\hookrightarrow B_2H_5 + BH$$

While at this stage we can select the major contributing processes that generate OH, clearly these are closely coupled to other concurrent reactions. For diborane much remains to be measured, to confirm the proposed mechanism. Monitoring species other than OH is essential. One should focus on the dominant species, listed in descending concentration levels HBO:($\sim 10^{-7}$ M), BO(10^{-7}), BH(10^{-8}), HBOH(7×10^{-9}), BO(10^{-9}), BH_2(10^{-9}) and OBOH(4×10^{-10}M).

These are predicted by the proposed mechanism for undiluted B_3H_6 injected into an excess of [O] at 7 Torr, total pressure.

ACKNOWLEDGMENTS

This program was supported, in part, by the U. S. Department of Energy, under contract DE-AC01-80 ER 10661.A004; the major portion of support was derived from ARO grant number DAAG29-84-K-0195. We thank Dr. C. F. Melius for providing his tables of computed ΔH°_{f}'s and S° prior to their publication.

REFERENCES

1. W. G. Berl, in Heterogeneous Combustion, Ed. H. G. Wolfhard, I. Glassman, and L. Green, Jr., Academic Press, New York, 1963, p. 311.
2. W. H. Bauer and S. E. Wiberley, 1958 report from Rensselaer Polytechnic Institute; Also, Advances in Chemistry, Series #32, ACS, 1961, p. 115, Ed. R. F. Gould.
3. C. W. Hand and L. K. Derr, Inorg. Chem. 13, 339 (1974).
4. G. K. Anderson and S. H. Bauer, J. Phys. Chem. 81, 29 (1977).
5. P. M. Jeffers and S. H. Bauer, Chem. Phys. Lett. 80, 29 (1982).
6. P. M. Jeffers and S. H. Bauer, J. Phys. Chem. 88, 5039 (1984).
7. A review summarizing the gas phase kinetics of boron and borane (S. H. Bauer) will shortly appear in a forthcoming volume, Molecular Structure and Energetics, Vol. 5, Ed. Liebman and Greenberg.
8. W. M. Shaub and M. C. Lin, NBS Special Publication #561, 1979, p. 1249.
9. N. Cohen and K. R. Westberg, Int. J. Chem. Kin. 18, 99 (1986).
10. a. J. T. Herron and R. E. Huie, J. Phys. Chem. Ref. Data 2, 467-518 (1973).
    b. R. E. Huie and J. T. Herron, Prog. React. Kin. 8, 1-80 (1975).
11. a. P. Andresen and A. C. Luntz, J. Chem. Phys. 72, 5842-5850 (1982).
    b. N. J. Dutton, I. W. Fletcher and J. C. Whitehead, Mol. Phys. 52, 475-483 (1984) found similar results for $O(^3P)$ with their cyclic hydrocarbons.
12. A. C. Luntz and P. Andresen, J. Chem. Phys. 72, 5851-5856 (1980).
13. a) R. Atkinson, et al., Advances in Photochemistry, Vol. 11, Ed. J. N. Pitts, Jr., G. S. Hammond and K. Gollnick, John Wiley & Sons, New York, 1979, pp. 375-488.

b) R. Atkinson, Int. J. Chem. Kin. 18, 555 (1986).

c) A. T. Droege and F. P. Tully, J. Phys. Chem. 90, 1949 (1986).

14. N. Cohen, Int. J. Chem. Kin. 14, 1339-1362 (1982).

15. R. W. Walker, Int. J. Chem. Kin. 17, 573-582 (1985).

16. a. M. L. Poutsma, in Methods in Free Radical Chemistry, Vol. I, Ed. E. S. Huyser, M. Dekker, New York, (1969), pp. 79-176.

b. G. C. Fettis and J. H. Knox, Prog. React. Kin. 2, 1-38 (1964).

17. N. Cohen, Int. J. Chem. Kin. 18, 57 (1986).

18. C. K. Westbrook and F. L. Dryer, Prog. Energy Combust. Sci. 10, 1 (1984).

19. N. J. Dutton, I. W. Fletcher, and J. C. Whitehead, J. Phys. Chem. 89, 569 (1985).

20. Thanks due to W. Braun, NBS, Gaithersburg, Maryland.

21. F. Westley, "Table of Recommended Rate Constants for Chemical Reactions Occurring in Combustion," *NSRDS-NBS #67*, 1980.

22. W. Tsang and R. F. Hampson, J. Phys. & Chem. Ref. Data 15, 1087 (1986).

23. J. W. Moore and R. G. Pearson, Kinetics and Mechanism, John Wiley & Sons, New York, 1981, Chapters 5 and 6.

24. C. F. Melius, Sandia National Laboratory (1987), private communication.

25. F. P. Fehlner and R. L. Strong, J. Phys. Chem. 64, 1522 (1960). [Insufficient data for estimating rate constants.]

TABLE I

A MINIMAL MECHANISM FOR C_2H_6 + O(^{3}P) REACTIONS [300 K; He 14 Torr]

#	REACTANTS				PRODUCTS			k(l/mole-s)	COMMENT
1	C2H6	+	O	=	C2H5	+	OH	2.00E06	(a) 1.74E05
2	C2H6	+	OH	=	C2H5	+	H2O	1.70E08	(a) 1.59E08
3	O	+	O	=	O2			2.90E05	(a) 2.84E05
4	O	+	OH	=	O2	+	H	2.30E10	a
5	O	+	OH	=	HO2			3.74E08	b
6	O	+	H	=	OH			1.18E07	a
7	O	+	O2	=	O3			1.52E05	negligible
8	O	+	HO2	=	OH	+	O2	3.40E10	(c) 3.75E10
9	H	+	OH	=	H2O			1.84E08	a {30}
10	H	+	H	=	H2			2.50E06	(a) 2.45E06
11	H	+	O2	=	HO2			1.60E07	(d) 7.06E06{31}
12	H	+	HO2	=	OH	+	OH	3.89E10	a
13	H	+	HO2	=	H2O	+	O	1.81E09	e
14	H	+	HO2	=	H2	+	O2	8.00E09	(e) 7.06E06{31}
15	H	+	O3	=	O2	+	OH	1.60E10	e
16	C2H5	+	O	=	CH3CHO	+	H	5.00E10	(a) 8.13E10
17	C2H5	+	O	=	HCHO	+	CH3	1.00E10	(a) 1.62E10
18	C2H5	+	H	=	C2H6 (h.p.l.)			4.00E10	(a) 3.61E10{32}
19	C2H5	+	H	=	CH3	+	CH3	2.00E10	(a) 2.7E09
20	CH3CHO	+	O	=	CH3CO	+	OH	3.00E08	b
21	CH3CHO	+	OH	=	CH3CO	+	H2O	1.00E10	(f) 6.02E09
22	CH3CO	+	O	=	CH3	+	CO2	3.00E10	b;(a) 9.6E09
23	CH3	+	O	=	H	+	HCHO	1.00E11	(a) 7.8E10{33}

TABLE I (Continued)

24	HCHO	+	OH	=	HCO	+	OH		1.00E08		a
25	HCHO	+	OH	=	H2O	+	HCO		5.60E09	(a)	6.09E09
26	HCHO	+	H	=	H2	+	HCO		4.00E07	(a)	3.46E07
27	HCO	+	O	=	OH	+	CO		6.30E10	(a)	3.0E10
28	HCO	+	O	=	H	+	CO2		4.00E10	(a)	3.0E10
29	HCO	+	H	=	H2	+	CO		6.60E10	(g)	8.43E10

a) Ref. 22 cited indicated value.

b) Ref. 21; we assume $k_{bi} = (1500/T)[He]$.

c) J. M. Nicovich and P. H. Wine, J. Phys. Chem. 91, 5118 (1987).

d) K. J. Hsu, J. L. Durant and F. Kaufman, J. Phys. Chem. 91, 1895 (1987).

e) D. L. Baulch, R. A. Cox, R. F. Hampson, Jr., J. A. Kerr, J. Troe and R. T. Watson, J. Phys. and Chem. Ref. Data 13, 1259.

f) Estimated from analogous reactions, cited in Ref. 13a.

g) R. S. Timonen, E. Ratajczak and D. Gutman, J. Phys. Chem. 91, 692 (1987).

Specifically, the following reactions were tested as to whether their inclusion affected $[OH]_t$, and found negligible.

{30}	OH	+	H	=	O	+	H2			(a)	6.32E04
{31}	O2	+	H	=	OH	+	O				2.1E-01
{32}	C2H5	+	H	=	C2H4	+	H2			(a)	1.81E09
{33}	CH3	+	OH	=	CH3OH					(a)	3.0E09 for 5-15 Torr He
{34}	OH	+	OH	=	H2O	+	O			(a)	1.21E09
{35}	OH	+	HO2	=	H2O	+	O2			(a)	4.82E10
{36}	OH	+	HCO	=	H2O	+	CO			(a)	3.01E10
{37}	OH	+	CH3O	=	CH2CO	+	H2O			(a)	1.2E10
				=	CH3	+	CO	+	OH	(a)	3.0E10
{38}	O	+	CH3O	=	CH2O	+	OH				1.0E10
				=	CH3	+	O2				1.0E10
{39}	HCO	+	HCO	=	H2CO	+	CO				5.0E10

TABLE II

Sensitivity Estimates for: $C_2H_6 + O(^3P)$

At: 300 K, with $[C_2H_6)_i$ = 3.22 E-06; $[O]_i$ = 2.35 E-06; 14 Torr total pressure

$$\frac{\partial[OH]_{ss}}{\partial k_i} \approx \frac{[R_i]_t}{k_4+k_5} \left[\frac{\text{mol } \ell^{-1}}{\text{mol}^{-1}\ \ell\ s^{-}}\right]$$

k_4 = 2.30 E10; k_5 = 3.74 E08; time/ms ——

(Reaction #) Reactant	1.73	→	3.47	6.94	13.9	20.8
(1) C_2H_6	1.36 E-16	→	1.35	1.34	1.31	1.31
(6) H	3.08 E-18	→	7.06	14.7	24.5	28.1
(8) HO_2	2.81 E-22	→	4.71	11.3	33.4	58.6
(20) CH_3CHO	5.26 E-19	→	6.59	6.59	5.43	4.49
(24) HCHO	0.63 E-18	→	1.30	2.07	2.38	2.25
(27) HCO	0.61 E-21	→	1.26	1.98	2.20	2.04

At: 300 K, with $[C_2H_6]_i$ = 8.3 E-07; $[O]_i$ = 1.46 E-06; 7 Torr total pressure

(Reaction #) Reactant	1.68	→	5.03	10.10	15.10
(1) C_2H_6	3.56 E-17	→	3.53	3.48	3.44
(6) H	0.44 E-18	→	1.71	3.95	6.17
(8) HO_2	2.81 E-23	→	4.83	8.94	15.5
(20) CH_3CHO	1.03 E-19	→	1.73	1.87	1.82
(24) HCHO	0.89 E-19	→	3.15	5.49	6.60
(27) HCO	0.86 E-22	→	3.06	5.29	6.31

TABLE III

MECHANISM FOR B_2H_6 + O(^{3}P) REACTIONS [350 K]

#	REACTANTS			=	PRODUCTS			k(l/mole-s)	COMMENT
1	B_2H_6	+	O	=	BH_3	+	H_2BOH	2.00E06	a
2	B_2H_6	+	O	=	B_2H_5	+	OH	9.75E06	a
3	B_2H_6	+	OH	=	H_2O	+	B_2H_5	9.75E09	
4	B_2H_5	+	O	=	BH_3	+	HBOH	3.20E09	
5	B_2H_5	+	H	=	B_2H_6			*1.00E11	
6	BO	+	H	=	HBO			*9.00E11	x
7	B_2H_5	+	OH	=	BH_3	+	H_2BOH	8.00E08	
8	H_2BOH	+	O	=	HBOH	+	OH	4.00E09	
9	H_2BOH	+	O	=	OBOH	+	H_2	6.50E07	
10	HBOH	+	O	=	HBO	+	OH	4.50E09	x
11	BH_3	+	BH_3	=	B_2H_6			*6.24E11	
12	BH_3	+	O	=	HBO	+	H_2	5.00E07	
13	H	+	HBO	=	HBOH			*1.50E08	
14	BH_3	+	OH	=	BH_2	+	H_2O	1.00E08	x
15	BH_2	+	O	=	HBO	+	H	1.00E09	x
16	HBO	+	O	=	BO_2	+	H	1.00E05	
17	HBO	+	OH	=	BO	+	H_2O	7.00E08	
18	HBO	+	OH	=	BO_2	+	H_2	7.00E08	
19	BH_3	+	O	=	BH_2	+	OH	5.00E09	x
20	OBOH	+	O	=	BO_2	+	OH	1.00E07	
21	BH_2	+	O	=	BH	+	OH	5.00E07	
22	BH_2	+	O	=	BO	+	H_2	5.00E10	
23	O_2	+	BH_3	=	HBOH	+	OH	3.00E06	b

TABLE III (Continued)

24	O_2	+	BH_2	=	HBO	+	OH	1.00E07	
25	O_2	+	BH	=	BO	+	OH	5.00E07	x
26	BO	+	OH	=	OBOH			*9.50E11	
27	BH	+	OH	=	{HBOH}BO	+	H_2	1.56E11	
28	O	+	O	=	O_2			*4.52E08	
29	OH	+	O	=	O_2	+	H	2.30E10	
30	OH	+	O	=	HO_2			*5.83E11	
31	H	+	O	=	OH			*1.84E10	
32	O_2	+	O	=	O_3			*2.37E08	
33	HO_2	+	O	=	O_2	+	OH	3.40E10	
34	H	+	OH	=	H_2O			*2.87E11	
35	H	+	H	=	H_2			*3.90E09	
36	O_2	+	H	=	HO_2			*2.50E10	
37	HO_2	+	H	=	OH	+	OH	3.89E10	
38	HO_2	+	H	=	H_2O	+	O	1.81E09	
39	HO_2	+	H	=	H_2	+	O_2	8.00E09	
40	H	+	O_3	=	O_2	+	OH	1.60E10	

* These rate constants (three-body associations) were multiplied by the ambient gas density to convert to bimolecular processes. k's for #28-#40 were transferred from Table I.

[a] The overall loss rate in this mechanism is 3.4 * that reported in Ref. 4.

[b] Consistent with upper limit of rate constant cited by L. Pasternack et al. (NRL Report, 1987).

[x] Adjusted from values proposed in Ref. 8. All others were estimated on basis of the magnitudes of their ΔG^0's and adjusted to obtain the indicated [OH] profiles.

ADJUNCT DATA

RELATIVE OH PRODUCTION LEVELS

During the development of the experimental unit to its present state, numerous runs were made in which C/H and B/H fuels were tested. While none of the following experiments was continued far enough to permit the development of a quantitative mechanism for the extended process,

$$\left.\begin{matrix} C/H \\ B/H \end{matrix}\right\} + O(^3P) \longrightarrow \ldots [OH] \ldots,$$

all the runs were quantitated relative to OH levels produced by C_2H_2 [or C_6H_{14}] + $O(^3P)$ under strictly comparable conditions. The measured values can be interpreted provided simplifying assumptions are introduced. The level of detail which can be derived therefrom vary from fuel to fuel, depending on the presumed complexities of the oxidation sequences of C/H or B/H to that of C_6H_{14} or C_2H_6.

TABLE AI (02/15/85)

Relative Rate Constants of Hydrogen Abstraction by $O(^3P)$

Reactions with Aromatic Hydrocarbons

$$RH + O \longrightarrow OH + R$$

	$\frac{k_{RH}}{k_{n\text{-hexane}}}$	k_a ($cm^3 mol^{-1} sec^{-1}$)
n-hexane	1.0	5.60×10^{10}
toluene	0.305	1.71×10^{10}
o-xylene	0.654	3.67×10^{10}
m-xylene	0.442	2.48×10^{10}
p-xylene	0.316	1.77×10^{10}
1,3,5-trimethylbenzene	1.292	7.24×10^{10}

1. J. T. Herron and R. E. Huie, J. Phys. Chem. Ref. Data 2, 467 (1973)

2. J. T. Herron and R. E. Huie, J. Phys. Chem. 73, 3327 (1969).

TABLE AII (02/15/85)

Branching Ratios of Hydrogen Abstraction to Overall Reaction of $O(^3P)$ with Aromatic Hydrocarbons

	$k(cm^3mol^{-1}sec^{-1})$			$\frac{k_a}{k_t}$	
	$RH + O \xrightarrow{k_t}$ product		$RH+O \xrightarrow{k_a} OH+R$		
	Ref 1	Ref 3	This Work	Ref 1	Ref 3
toluene	1.4×10^{11}	0.45×10^{11}	1.71×10^{10}	0.12	0.38
o-xylene	6.7×10^{11}	1.05×10^{11}	3.67×10^{10}	0.05	0.35
m-xylene	7.7×10^{11}	2.12×10^{11}	2.48×10^{10}	0.03	0.12
p-xylene	4.5×10^{11}	1.09×10^{11}	1.77×10^{10}	0.04	0.16
1,3,5-trimethylbenzene	2.24×10^{12}	1.68×10^{12}	7.24×10^{10}	0.03	0.04

3. R. Atkinson and J. N. Pitts, Jr., J. Phys. Chem. 78, 1780 (1974); 79, 3327 (1975).

TABLE AIII (05/25/85)

Relative Rate Constants of Hydrogen Abstraction by $O(^3P)$ from C_2H_2 and C_2H_4

[Deduced branching ratios]

n-hexane	k_{total} (ref. 1) $cm^3\ mole^{-1}\ s^{-1}$	$k_{abstraction}$ *	Branching ratio k_a/k_t
n-hexane	5.6×10^{10}	$[5.6 \times 10^{10}]$	[1]
C_2H_4	9.5×10^{10}	4.38×10^{9}	0.046
C_2H_2	4.9×10^{11}	2.10×10^{10}	0.043

* Deduced from [OH] levels relative to that generated by n-hexane under identical conditions.

TABLE AIV

THERMOCHEMICAL PARAMETERS

(Gas phase; 1 atmosphere; 298°K)

Source: C. F. Melius, Sandia National Laboratory (2/18/87)

Species	ΔH_f° (kcal/mole)	S° (e.u.)		Species	ΔH_f° (kcal/mole)	S° (e.u.)	
B	133.8	36.65		H	52.10	27.39	*
B_2	195.0	48.23	*	BH	106.6	41.05	
BO	- 0.7	48.60		BH_2	75.7	43.04	
BO_2	- 62.0	54.90		BH_3	23.2	44.88	
HBO	- 58.5	50.24		B_2H_6	[48]	[53]	
HBOH	- 15.8	[56]		B_2H_4	9.8	55.71	
H_2BOH	- 68.5	[57]		B_4H_9	17.5	65.80	*
H_2BO	- 13.3	[54]		$B_{10}H_{14}$	11.3	84.15	*
OBOH	-131.8	57.27					
$B(OH)_2$	-102.0	58.12		CO	- 26.4	47.21	*
$BH(OH)_2$	-157.3	[60]		PF_3	-224.9	65.28	*
B_2O	23.0	54.40	*	$N(CH_3)_3$	- 5.7	69.02	a
B_2O_2	-115.0	57.96		H_3BCO	- 26.5	59.69	a
B_2O_3	-199.6	67.80		H_3BPF_3	-225.6	74.54	a
$B_2(OH)_4$	-307.0	83.37		H_3BNMe_3	- 20.4	[77]	a
$B(OH)_3$	-237.2	70.54					

* - JANAF - 2nd Ed; [ ] - estimated; a - other sources

LEGENDS FOR FIGURES

Figure 1: Schematic of apparatus.

Figure 2: [OH] observed (O & ⬡) and calculated *via* the mechanism listed in Table I (300 K).

Figure 3: [OH] observed (O & ⬡) and calculated *via* the mechanism listed in Table III (350 K).

Figure 4: *Preliminary*: relative production levels of [OH] for B_2H_6, H_3BCO and B_4H_9.

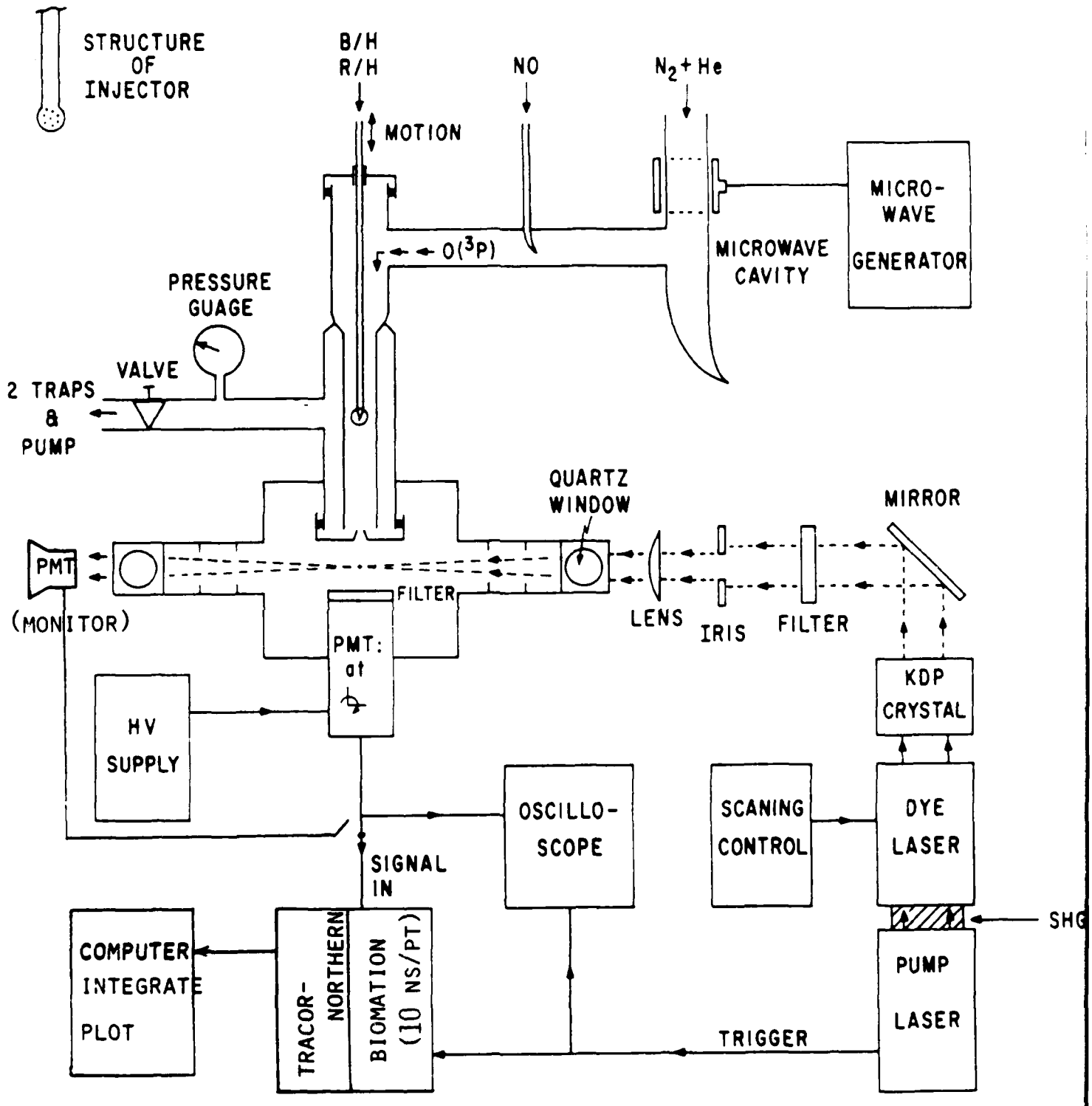
STRUCTURE OF INJECTOR
B/H
R/H
NO
N_2 + He
MOTION
MICRO-WAVE GENERATOR
MICROWAVE CAVITY
O(^{3}P)
PRESSURE GUAGE
VALVE
2 TRAPS & PUMP
QUARTZ WINDOW
MIRROR
PMT
(MONITOR)
FILTER
LENS
IRIS
FILTER
PMT: at
HV SUPPLY
KDP CRYSTAL
OSCILLO-SCOPE
SCANING CONTROL
DYE LASER
SIGNAL IN
SHG
COMPUTER INTEGRATE PLOT
TRACOR-NORTHERN
BIOMATION (10 NS/PT)
PUMP LASER
TRIGGER

FIGURE 1

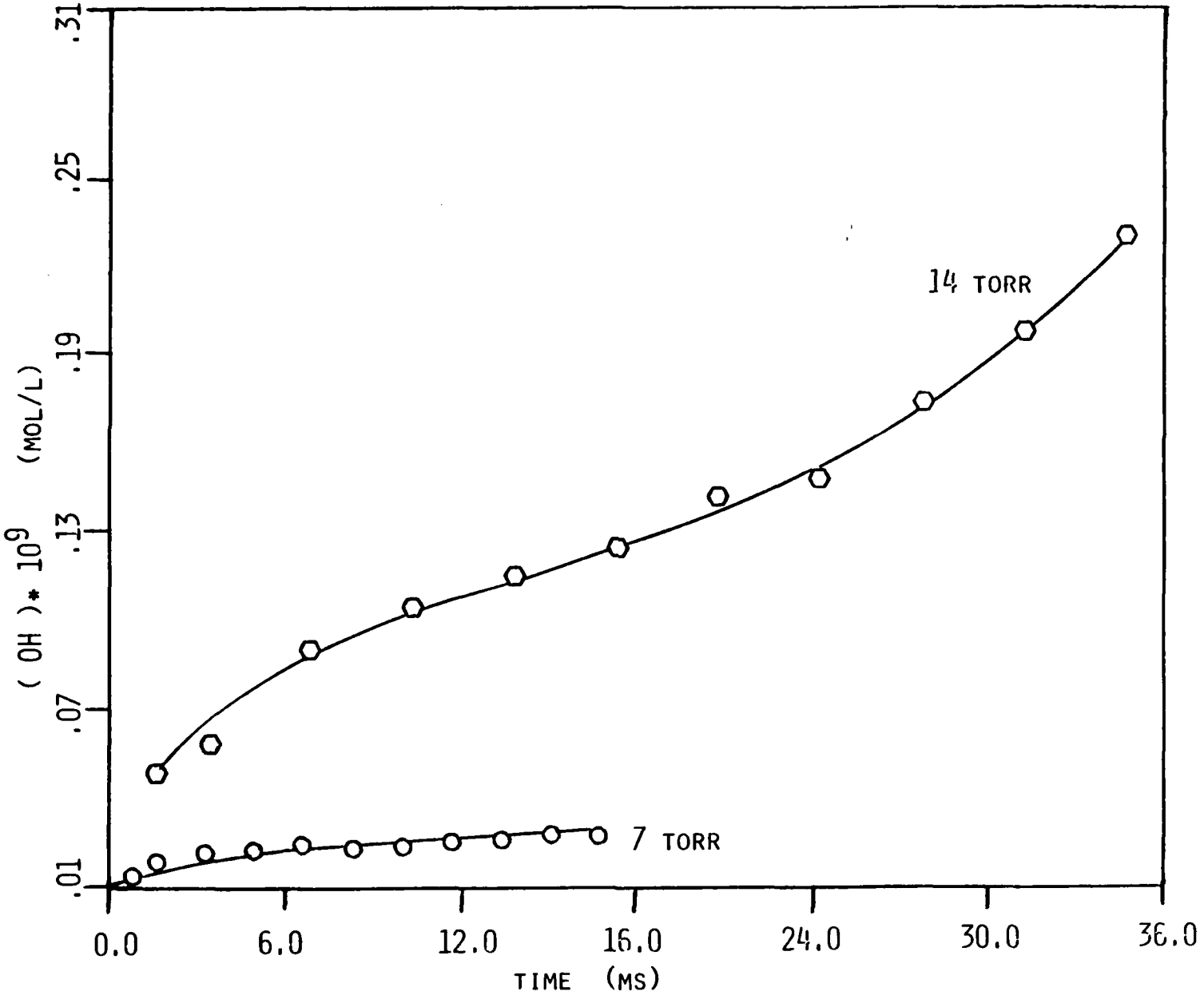
.31
.25
.19
.13
.07
.01
(OH)* 10^9 (MOL/L)
14 TORR
7 TORR
0.0
6.0
12.0
16.0
24.0
30.0
36.0
TIME (MS)

FIGURE 2

FIGURE 3

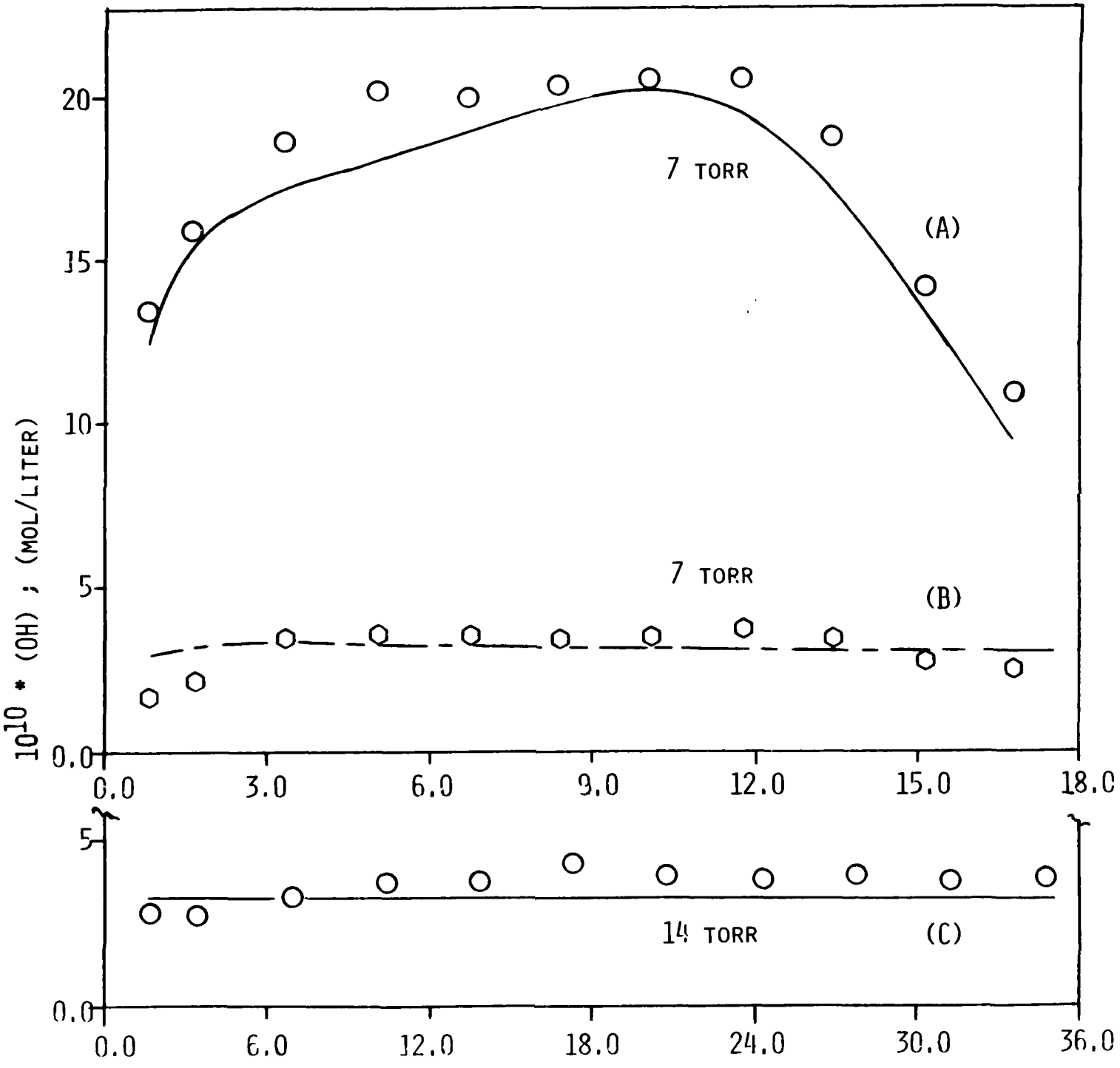
20
15
10
5
0.0
10^{10} * (OH) ; (MOL/LITER)
7 TORR
(A)
7 TORR
(B)
0.0
3.0
6.0
9.0
12.0
15.0
18.0
5
0.0
14 TORR
(C)
0.0
6.0
12.0
18.0
24.0
30.0
36.0

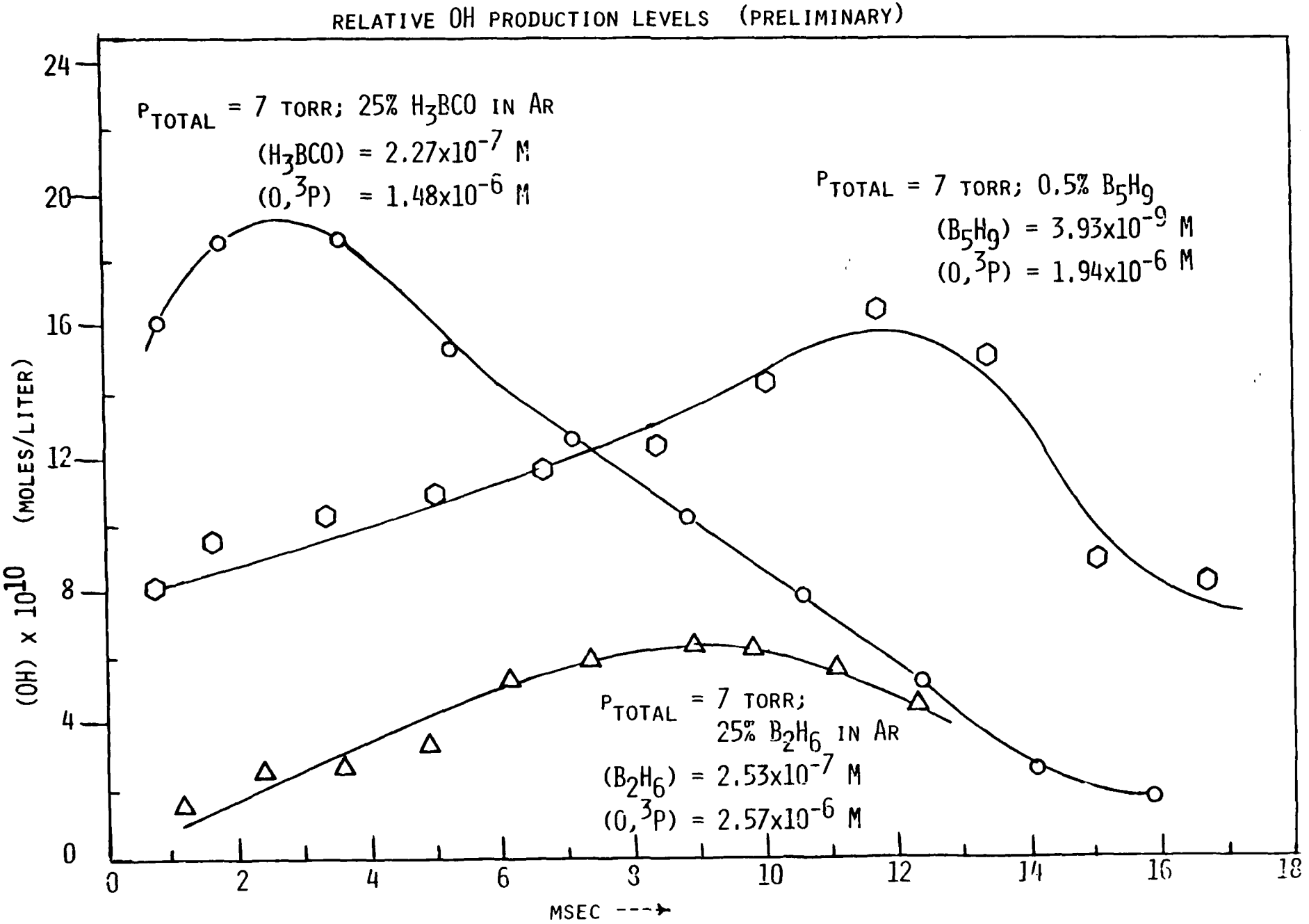
RELATIVE OH PRODUCTION LEVELS (PRELIMINARY)
P_{TOTAL} = 7 TORR; 25% H_3BCO IN AR
(H_3BCO) = 2.27×10^{-7} M
$(O,^3P)$ = 1.48×10^{-6} M
P_{TOTAL} = 7 TORR; 0.5% B_5H_9
(B_5H_9) = 3.93×10^{-9} M
$(O,^3P)$ = 1.94×10^{-6} M
P_{TOTAL} = 7 TORR;
25% B_2H_6 IN AR
(B_2H_6) = 2.53×10^{-7} M
$(O,^3P)$ = 2.57×10^{-6} M
(OH) x 10^{10} (MOLES/LITER)
0
4
8
12
16
20
24
0
2
4
6
3
10
12
14
16
18
MSEC --->

FIGURE 4

END
DATE
FILMD
3-88
DTIC